Absorption, luminescence and scattering of single nano-objects

Yorulmaz, M.

CHAPTER 5

Luminescence quantum yield of single gold nanorods

We study the luminescence quantum yield (QY) of single gold nanorods with different aspect ratios and volumes. Compared to gold nanospheres, we observe an increase of QY by about an order of magnitude for particles with a plasmon resonance >650 nm. The observed trend in QY is further confirmed by controlled reshaping of a single gold nanorod to a spherelike shape. Moreover, we identify two spectral components, one around 500 nm originating from a combination of interband transitions and the transverse plasmon and one coinciding with the longitudinal plasmon band. These components are analyzed by correlating scattering and luminescence spectra of single nanorods and performing polarization sensitive measurements. Our study contributes to the understanding of luminescence from gold nanorods. The enhanced QY we report can benefit applications in biological and soft matter studies.

The contents of this chapter are based on:
M. Yorulmaz, S. Khatua, P. Zijlstra, A. Gaiduk, and M. Orrit, "Luminescence quantum yield of single gold nanorods", Nano Lett. **12**, 4385-4391 (2012)

5.1 Introduction

Optical probes that provide good contrast and are small enough not to perturb the system under investigation are essential to obtain structural and dynamical information on the nanoscale. For this purpose, single fluorescent molecules are widely used as probes of, for instance, soft matter systems[24,47,48,203] and biological mechanisms[45,46] since they are small and have a high fluorescence quantum yield. However, single molecules suffer from blinking[51] and bleaching,[53] which limits their observation time.

Gold nanoparticles do not blink nor bleach and their nontoxicity and biocompatibility make them attractive for biological applications.[11,28] There has been a considerable effort to investigate their size- and shape-dependent optical properties, both experimentally[32,156] and theoretically.[72,73] Their scattering and absorption properties have been widely investigated and characterized, which has led to many new applications.[71]

In recent studies, the photoluminescence from single gold nanoparticles has proven to be a complementary property to absorption and scattering for imaging and sensing purposes.[192,204–207] Although the luminescence quantum yield (QY) of gold nanoparticles is several orders of magnitude lower than the QY of fluorescent labels such as organic dyes or semiconductor nanoparticles, their large absorption cross section compensates for their low QY, making them high-contrast imaging agents.

The first observation of photoluminescence of gold dates back to 1969, when Mooradian studied bulk gold[208] and observed a broad luminescence spectrum with a QY of about 10^{-10}. Photoluminescence from bulk gold originates from radiative transitions of conduction electrons toward empty electron states, which can be either holes in the d-band (electron-hole interband recombination),[208–211] or empty electron states or holes within the sp-conduction band (intraband transitions).[182]

Later, the effect of surface roughness on the photoluminescence of gold was studied by Boyd et al. who showed that the QY could be enhanced by several orders of magnitude compared to a smooth film.[210] The enhancement was attributed to the concentration of fields at tips of surface protrusions (lightning-rod effect) and to the presence of localized surface plasmons.[210,212] Since this first observation of plasmon-enhanced emission, the effect of localized surface plasmons has been investigated in solutions of nanoparticles

with different sizes and shapes.

Early efforts to understand the emission from gold nanoparticles have relied on ensemble measurements. A QY of $\sim 10^{-5}$ to 10^{-4} was reported for ensembles of 5 nm diameter gold nanospheres by Wilcoxon et al.[186] Mohammed et al.[213] have measured the luminescence from ensembles of gold nanorods with aspect ratios ranging from 2.4 to 5.4 and reported QYs of 10^{-4}-10^{-3}. They have explained the observed luminescence by the radiative recombination of electron-hole pairs that is enhanced by local fields associated with the particle plasmon resonance. In a recent ensemble study by Dulkeith et al., the QY of gold nanospheres with diameters ranging from 2 to 60 nm was reported to be $\sim 10^{-6}$ and independent of size.[180] These authors argued that the moderate field enhancement of about 10 was too weak to explain this enhancement by 4 orders of magnitude compared with bulk gold. Instead of the radiative recombination of e-h pairs, the authors proposed a process in which d-band holes recombine non-radiatively with sp electrons. In the process, each excited d-band hole polarizes the particle and thus triggers a collective electron oscillation, that is, a surface plasmon. These plasmons decay either radiatively by emitting photons or nonradiatively via transformation into excited e-h pairs.

The reported QYs of gold nanoparticles in ensemble measurements differ by 2-3 orders of magnitude. The observed variations could be due to the presence of inhomogeneities within the sample. For instance, the measured signal can be easily overestimated due to a low number of aggregates of nanoparticles. Other measurements may have been affected by reabsorption of luminescence, which reduces the apparent signal. This complicates the interpretation of ensemble studies and manifests the need for single-particle measurements.

Gaiduk et al.[156] reported the luminescence QY of single gold nanospheres to be $\sim 3 \times 10^{-7}$ on average and independent of size for diameters ranging from 5 to 80 nm, which is in agreement with the measurements of Dulkeith et al.[180] Recently, one-photon plasmon luminescence from individual nanorods has been studied by Tcherniak et al.[206] They showed that plasmons play a central part in the observed luminescence from nanorods, because the luminescence spectrum closely reproduces the sharp plasmonic band of the scattering spectrum. The same group reported the QY of a single gold nanorod of 24 nm $\times$ 76 nm to be 8×10^{-6} when excited at 514 nm. This measured QY is

significantly higher than the QY reported by Gaiduk et al.[156] for single gold nanospheres. However, no explanation was proposed for the larger QY of nanorods and its shape dependence.

The reported luminescence QY for nanoparticles with different sizes and shapes range from 10^{-7} to 10^{-4} in the above-mentioned studies.[156,180,186,206,213] Although it was shown that the QY is roughly independent of size for nanospheres, further experiments are required to establish the effects of the particle shape. These studies could shed light on the mechanism of the luminescence, which will benefit potential applications.

In this chapter, we present a detailed study of the luminescence QY of single gold nanoparticles of different shapes and sizes. We systematically study nanorods with aspect ratios ranging from 1 (sphere) to 3.5. We show about an order of magnitude increase in QY for nanorods with longitudinal plasmon wavelengths longer than 650 nm compared to spheres. The observed trend is confirmed when a single gold nanorod is slowly reshaped to a spherelike shape. We find a strong correlation between the scattering and luminescence spectra of the same particle, confirming the plasmonic influence on the observed luminescence. Finally, we investigate the luminescence spectrum of a nanorod by performing polarization-sensitive measurements. We show that the emission is dominated by a polarized contribution that coincides with the longitudinal plasmon. In addition, we consistently observe a weak short-wavelength component that peaks around 500 nm and is not (or only weakly) polarized. We attribute this component to a combination of interband transitions and the transverse surface plasmon.

5.2 Experimental

5.2.1 Sample preparation

We prepared gold nanorods with different sizes by varying the silver ion and seed concentration in a seed-mediated growth method.[214] Electron microscopy images and the dimensions of the nanorods used in this study are shown in Fig. 5.1. The extinction spectra of the nanorod suspensions are shown in Appendix D (Fig. D.1), where longitudinal SPRs at around 630, 650 and 730 nm are observed for nanorods with ensemble-averaged aspect ratios of 2.4, 2.6 and 3.4, respectively. In addition, we used a commercial col-

loidal suspension of 18.5 nm diameter[156] gold nanospheres (British Biocell International).

For the optical experiments we spin-coated gold nanoparticles on a clean glass substrate and used glycerol as immersion liquid. We obtained samples with well-separated nanoparticles so that single particles could be optically resolved.

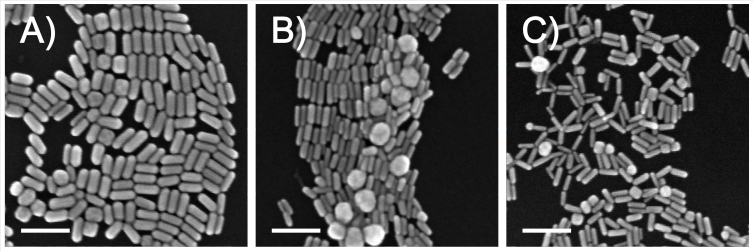

sample	length (nm)	width (nm)	asp. ratio	V (10^3 nm^3)
A	58±5	25±4	2.4±0.4	24±7
B	34±5	13±3	2.6±0.5	4±2
C	38±3	11±1	3.4±0.3	4±1

Figure 5.1: SEM images of the three samples used in this study. The table shows the dimensions of nanorods for each sample with standard deviations of the mean. Scale bars are 100 nm.

5.2.2 Optical microscopy

We performed single particle measurements on our home-built combined photothermal, scattering, and luminescence microscope, assembled on an inverted optical microscope (Olympus IX-71). Our photothermal microscope is described in detail elsewhere (see Chapter 2).[90] The schematic of the setup and the experimental details for combined photothermal (absorption) and fluorescence microscopy are given in Section 3.2.1. Details of combined fluorescence and scattering microscopy are discussed in Appendix D (Fig. D.2). Briefly, the continuous wave (cw) excitation light is time-modulated and overlapped with a cw probe beam that is off-resonance with the plasmon. Both excitation and probe lasers are focused through a microscope objective onto the sample. The energy absorbed by the particle is mainly released as heat giving rise to a temperature gradient ΔT_{surf} around the nanoparticle (Appendix D, Fig. D.3). The probe laser is scattered by the resulting refractive

index profile. This scattered field interferes with the reflected field creating small changes in the detected probe intensity. A lock-in amplifier demodulates the signal and provides the photothermal signal.

Photothermal microscopy provides contrast only for absorbing objects and suppresses scattering background from impurities or interfaces. The photothermal signal is proportional to the absorption cross section and in turn to the volume of the nanoparticle for a given excitation wavelength. To obtain the absolute absorption cross section of single nanorods we used gold nanospheres with a diameter of 18.5 nm as a calibration sample.[156] When the nanorods and nanospheres are imaged under the same illumination conditions the absorption cross section of a nanorod follows from:

$$\sigma_{\mathrm{NR}} = \sigma_{18.5} \times \frac{S_{\mathrm{NR}}}{S_{18.5}} \tag{5.1}$$

where σ_{NR} is the absorption cross section of the nanorod, $\sigma_{18.5}$ (calculated using full Mie theory[72] to be 203 nm^2 at 476 nm) is the absorption cross section of a single 18.5 nm diameter gold nanosphere, S_{NR} is the measured photothermal signal of a nanorod, and $S_{18.5}$ is the measured average photothermal signal of 18.5 nm spheres.

We chose 476 nm laser light (circularly polarized) as the excitation wavelength for both photothermal and luminescence imaging and an off-resonant 864 nm laser light as probe laser for photothermal microscopy. We sequentially recorded luminescence and photothermal images of the same particles at the same excitation intensity. With Eq. 5.1, the photothermal signal directly gives the measured absorption cross section at 476 nm, which was used to calculate the luminescence QY. Note that this method takes into account all factors that govern the absorption cross section of a particle such as defects, shape irregularities, and variations in local environment. These factors are difficult to take into account in calculations.

5.3 Results and discussion

We show typical photothermal and luminescence raster scan images of isolated nanorods with an ensemble-averaged aspect ratio of 2.4 in Fig. 5.2 A,B. Both images were recorded on the same area. The color scales of photothermal and luminescence image show the calculated absorption cross section

and luminescence count-rate. To confirm that each bright spot corresponds to a single gold nanorod, we recorded luminescence spectra of each particle, shown in Fig. 5.2 C. A single Lorentzian line-shape confirms that each spot corresponds to an individual nanorod. We observe a large spread in plasmon energy which is consistent with the presence of a broad distribution of aspect ratios as observed in electron microscope images (Fig. 5.1). Aggregates are easily identified in the spectra by a broadened or split peak[31] (Appendix D, Fig. D.4). Signals of such particles were discarded from the data analysis. We also checked that the plasmon resonance and the spectral line shape of each individual particle did not change after all measurements were finished. A typical example of these control experiments is shown in Appendix D (Fig. D.5). In order to check if the observed luminescence is a one-photon process, we measured the power dependence of the luminescence intensity. Indeed, the luminescence intensity was linearly dependent on the excitation laser power as shown in Appendix D (Fig. D.6). The excitation power dependence of the photothermal signal also exhibits a linear dependence, as expected[90] (Appendix D, Fig. D.6).

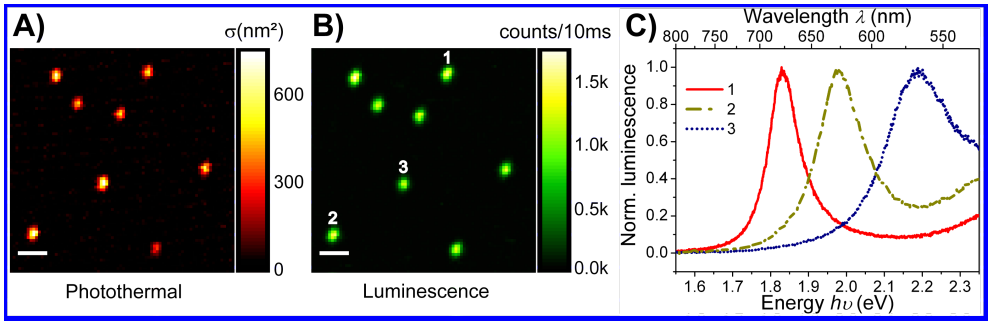

Figure 5.2: (A) Photothermal and (B) one-photon luminescence images of individual gold nanorods on a glass coverslip, immersed in glycerol. The scale-bars are 1 μm. (C) Normalized luminescence spectra of the numbered particles in panel B. Experimental: the excitation intensity is $I_{\text{exc}} = 32\ \text{kW/cm}^2$ (circularly polarized) for photothermal and luminescence images and luminescence spectra; the probe intensity is $I_{\text{probe}} = 1.4\ \text{MW/cm}^2$ to record photothermal images; acquisition and lock-in integration times for luminescence and photothermal images are $t_{\text{acq}} = 10$ ms and $t_{\text{int}} = 3$ ms, respectively. Each luminescence spectrum was recorded in 10 s.

The QY of individual nanorods was calculated from the signal strength in the photothermal and photoluminescence images. The photothermal sig-

nal was first converted into an absorption cross section, according to Eq. 5.1. Then, the luminescence count-rate of each single nanorod was used to calculate the QY[56,156] as follows:

$$\eta_{\mathrm{lum}} = \frac{N_{\mathrm{em}}}{N_{\mathrm{abs}}};\ N_{\mathrm{em}} = \frac{N_{\mathrm{signal}}}{\Pi_{\mathrm{setup}}};\ N_{\mathrm{abs}} = \frac{\sigma_{\mathrm{NR}} I_{\mathrm{exc}}}{h\nu_{\mathrm{exc}}} \tag{5.2}$$

where η_{lum} is luminescence QY, N_{em} is the number of emitted photons, N_{abs} is the number of absorbed photons, N_{signal} is the measured luminescence count-rate, Π_{setup} is the wavelength-dependent detection efficiency of the setup (Appendix D, Fig. D.7), σ_{NR} is the absorption cross section of the nanorod (obtained from the photothermal signal), I_{exc} is the excitation laser intensity and $h\nu_{\mathrm{exc}}$ is the photon energy of the excitation light. We estimate the error, $\delta\eta_{\mathrm{lum}}/\eta_{\mathrm{lum}}$, in the measured QYs to be 30%, taking into account the individual errors in the variables used for the QY calculation (Eq. 5.2).

In Fig. 5.3 we show the measured QY for individual nanorods with aspect ratios ranging from 1 to ∼3.5, or plasmon wavelengths ranging from 530 to 780 nm. The experiments were performed on 150 nanorods from the three samples shown in Fig. 5.1. We observe a significant increase in QY for particles with a plasmon between 530 and 650 nm. For nanorods with a plasmon resonance beyond 650 nm we observe no significant change in QY anymore.

The QY increase for longer nanorods with a plasmon moving from 530 to 650 nm may be correlated with the decreased damping of the plasmon by creation of interband excitations. The higher aspect ratio nanorods emit further away from the interband transitions. As the surface plasmon moves away from the interband transitions, less channels are available for dissipation, which raises the efficiency of radiative emission.[89] It is thus the proximity of the interband transitions to the plasmon resonance frequency that determines the QY. For nanorods with a plasmon energy lower than 1.8 eV,[215] creation of interband excitations is impossible and radiative emission only competes with the creation of intraband excitations.

It is important to note that the observed increase in QY is not caused by (photo)chemistry-mediated enhancements as we observed before on strongly excited gold nanospheres[155] (see Section 4.3.4). We reported a nonreversible enhancement in luminescence of gold nanospheres when the surface temperature of the nanoparticles was raised by 60 K.[155] The increase in luminescence was explained by modification of the surface of the nanoparticle, caused

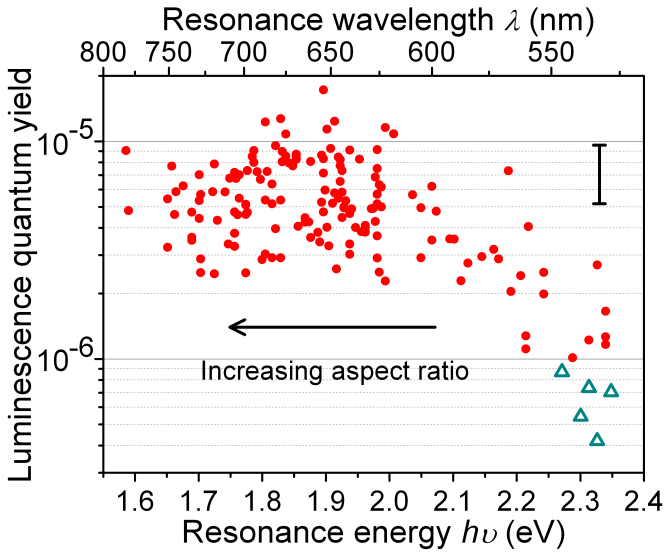

Figure 5.3: Luminescence QY of individual nanorods as a function of their plasmon resonance energy (red-filled circles). Data shown with open-dark-cyan triangles are from 18.5 nm diameter spheres and shown for comparison. Each individual dot here represents one particle. The arrow in the graph indicates the direction of increase of the nanorod aspect ratio. The error bar represents the estimated error in the QY measurement.

by thermal processes, photochemical processes, or a combination of both. To eliminate these effects we kept the surface temperature rise below 10 K by employing a low excitation intensity (for more details see Appendix D, Fig. D.3).

The QY of nanospheres was shown to be roughly independent of their size.[156] In order to establish the effect of the volume of a nanorod on its QY, we selected particles with similar plasmon energies but with different volumes (i.e., photothermal signal) from the data points in Fig. 5.3. We observe no significant dependence of the QY on volume (Appendix D, Fig. D.8). However, there is a slight decrease in QY for nanorods with larger volumes, as we also observed before for spheres[156] (see Chapter 4, Section 4.3.3). We hypothesize that the quantum yield may be lowered by reabsorption of radiation within the larger particles. The origin of this slight decrease is unknown and requires further investigation.

Figure 5.3 indicates a broad distribution of QYs, even for particles with

a similar plasmon energy. For example, particles with a plasmon between 620 and 630 nm exhibit QY values that range from 2.3×10^{-6} to 1.2×10^{-5}. We attribute this spread in QY to local irregularities in crystal structure, to faceting of particle surfaces, and/or to the possible presence of defects on the surface of the nanorods. In addition, small variations in the particle environment due to a molecular-scale contamination can cause these distributions. We cannot rule out the effect of small variations in the detection efficiency for different polarizations, which, among other mentioned reasons, could cause variations in the observed QY due to the random orientation of the particles on the sample surface.

Reshaping, the laser-induced shape transformation of a nanorod toward a spherical shape, can occur at temperatures well below the melting point of bulk gold (1064°C).[68,216,217] This allows us to compare the QY on one-and-the-same particle for different plasmon energies. For that purpose, we controllably reshaped a single gold nanorod in several steps, and measured its QY after each reshaping step. The reshaping was done by heating the particle with a circularly polarized 514 nm cw laser with powers ranging from 2 to 5 mW at the sample. These powers raise the particle's temperature by up to $\Delta T_{\text{surf}} \sim 160\ K$, resulting in a slow reshaping of the nanorod and a gradual blue shift of its plasmon resonance. We increased the excitation laser power and irradiation time as the nanorod's shape became more and more spherical in order to compensate for the increased thermal stability of lower aspect ratio particles.[69] The photothermal signal did not change significantly during the transformation of the nanorod to a sphere-like shape. This observation confirms that the volume of the particles is maintained.

The result of the thermal reshaping of the nanorod with an initial plasmon at 720 nm is shown in Fig. 5.4 where the QY of the nanorod is plotted as a function of its plasmon resonance after each reshaping step. Figure 5.4 clearly shows no significant change of QY when the plasmon resonance shifts from 720 to 640 nm. Further melting the particle shifted its plasmon to 540 nm and its QY reduced by a factor of 6. These results confirm the overall trend of QY that we observed in Fig. 5.3

We note that, even though the surface temperature increase was up to $\sim$160 K in this experiment, we did not observe any photoinduced luminescence as we reported before for citrate-capped gold spheres (see Chapter 4, Section 4.3.4).[155] In this study, we employed CTAB-coated gold nanorods,

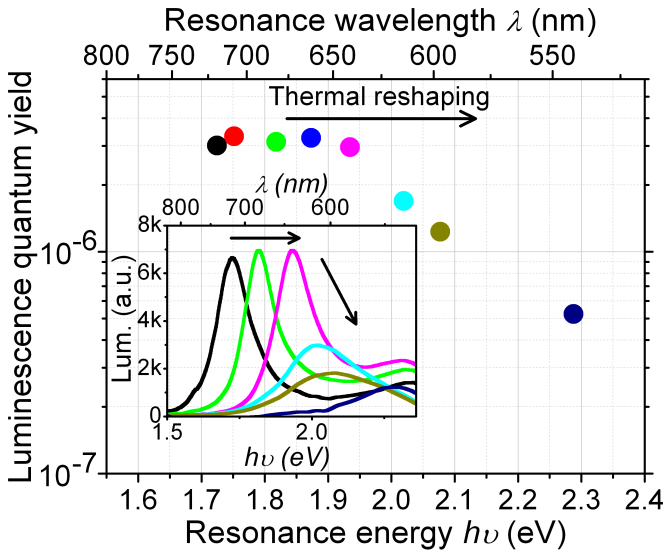

Figure 5.4: Controlled photothermal reshaping of a single gold nanorod. Each dot represents the QY of the same nanorod obtained after each thermal reshaping step as a function of its resonance energy. The inset shows the luminescence spectra of the nanorod after each reshaping (melting) step. Arrows in the graph indicate the direction of spectral and intensity change upon melting of the nanorod.

which were UV/ozone cleaned before the experiment to remove all organic molecules from the surface. The absence of the organic capping layer eliminates the photoinduced luminescence and allowed us to employ higher excitation powers.

In order to investigate the origin of the observed luminescence, we correlated the luminescence and the scattering spectra of the same particle. The results of these experiments are shown in Fig. 5.5. Figure 5.5 A,B shows luminescence and scattering images recorded on the same sample area. The luminescence spectra (green dots) correlate very well with the scattering spectra (blue lines) in Fig. 5.5 C, confirming the plasmonic origin of luminescence as previously reported.[180,182,217] We further confirmed the correlation between luminescence and scattering spectra by changing the medium around the same gold nanorod from air to glycerol, which caused a shift of both the scattering and the luminescence bands from 625 to 680 nm (Appendix D, Fig. D.9).

We note that there is a slight difference between photoluminescence and

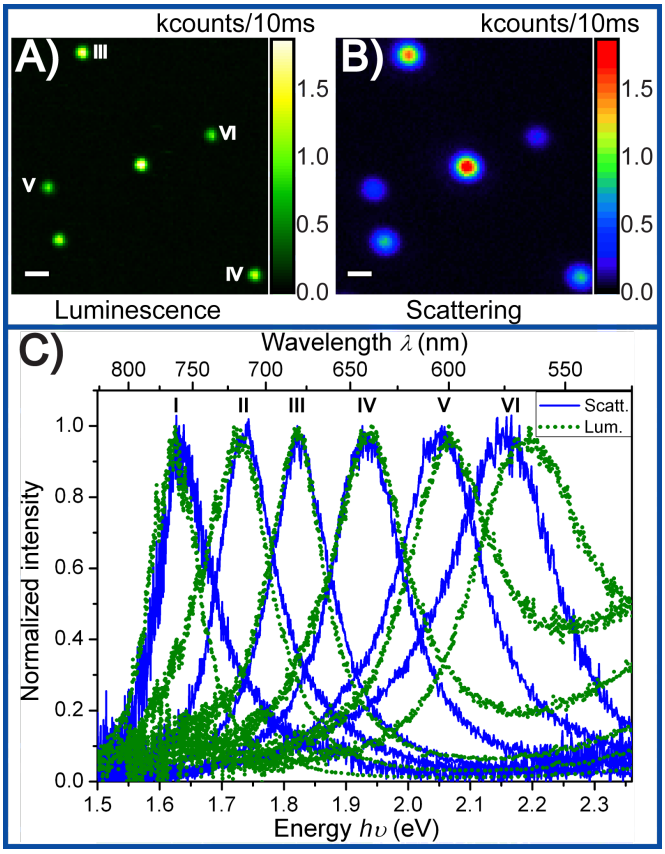

Figure 5.5: Correlation of scattering and luminescence spectra of individual gold nanorods with different aspect ratios. (A) Photoluminescence and (B) dark-field scattering image of gold nanorods with ensemble average aspect ratio of ∼2.4 taken on the same area of the sample. Scale bars correspond to 1 μm. (C) Correlation of normalized luminescence (green dots) and normalized scattering (blue line) spectra for nanorods with different aspect ratios. Photoluminescence signals were obtained with circularly polarized excitation at 476 nm and scattering signals were obtained by excitation with unpolarized white light. Particles I and II are measured from a different sample with an ensemble average aspect ratio of ∼3.4 to cover a larger wavelength range.

scattering spectra both in terms of peak position as well as the line-shape. This slight difference is especially apparent for nanorods with a lower aspect ratio (shorter resonance wavelength). Luminescence spectra appear broader as well as slightly blue shifted. Part of the shift may be due to a broad back-

ground ("green" emission), starting at about 690 nm (energy 1.8 eV) and increasing for shorter waves, which overlaps with the longitudinal plasmon of the shorter rods (see Fig. 5.5).

We further investigated the green component of the emission. By correlating its intensity with the photothermal signal for many individual particles, we found that this component is proportional to the volume of the nanorod (Appendix D, Fig. D.10). We then performed the polarization measurements presented in Fig. 5.6. To reduce depolarization effects by the microscope objective we decreased the excitation and collection NA to approximately 0.9. The right inset of Fig. 5.6 shows that the longitudinal plasmon component is strongly polarized, as expected for a dipolar emission pattern. In contrast, we did not observe any clear polarization of the green emission. This observation suggests that this component cannot be exclusively due to the transverse plasmon, which should be polarized along the short axis of the particle. The polarization anisotropy is a measure for the degree of polarization of the emission and is defined as

$$P = \frac{I_{\parallel} - I_{\perp}}{I_{\parallel} + I_{\perp}} \tag{5.3}$$

where $I_{\parallel}$ and $I_{\perp}$ are the emission intensities with an analyzer along the long and short axis of the nanorod, respectively. P is 0.9 for the longitudinal plasmon. We find $P = 0.1$ for the green component indicating a nearly unpolarized emission.

The green component we observe is peaked close to 500 nm, similarly to the luminescence of a smooth gold film measured by Beversluis et al.,[182] which they attributed to interband transitions (between d-band and sp-conduction band near the X and L points in the Brillouin zone). Any unpolarized interband emission should be enhanced by the transverse plasmon, as it happens for spheres. Some residual enhancement by the longitudinal plasmon may explain the absence of a clear polarization of the green component. Further studies are required to clarify this point.

Finally, we would like to discuss what our observations may tell us about the mechanism of the photoluminescence of gold nanoparticles. Two models have been proposed in the literature.

(i) The first model, based on energy transfer, postulates that the energy from an electron-hole pair is transferred to a plasmon excitation, which then

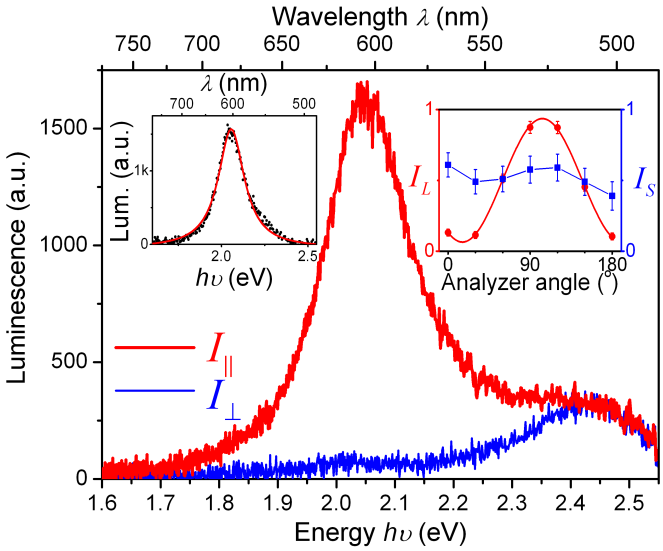

Figure 5.6: Luminescence spectra of a gold nanorod excited by a circulary polarized 476 nm laser beam and recorded with a detection polarizer parallel ($I_{\parallel}$, red) and perpendicular ($I_{\perp}$, blue) to the long axis of the nanorod. Left inset shows the longitudinal component of the luminescence spectrum (black dots) that is obtained after subtracting the luminescence spectrum perpendicular to the long-axis of the nanorod and the Lorentzian-line fit (red). Right inset shows the detection polarization dependence of the long wavelength peak (I_L, red dots) and the short wavelength peak (I_S, blue dots).

emits a photon.[23,180,217] The molecular analog is a FRET process, in which a virtual photon from the donor is absorbed by the acceptor, relaxes, and is re-emitted as acceptor fluorescence by the acceptor dipole moment.

(ii) The second interpretation involves the internal field enhancement, which in nanorods ranges from ten to a hundred.[218] The optical field created by the recombination is shared by the plasmon and enhanced by its antenna effect, enhancing the emission rate[182,213,219] (for gold particles excited at wavelengths shorter than 500 nm, no excitation enhancement is expected, and only luminescence enhancement can occur). The molecular analog of this mechanism is the emission of an exciton, a strongly coupled pair of molecules. The emission of the coherent exciton state proceeds via the collective dipole moment of the pair, not that of the acceptor alone.

In both cases, the luminescence is mainly determined by the plasmon's

dipole moment, either because the plasmon itself emits (model i) or because the plasmon's dipole moment is much larger than that of the original source, and because the enhancement factor resonates at the plasmon frequency (model ii). Therefore, the mere observation of the plasmon band in the luminescence spectra does not allow us to discriminate between the two models.

5.4 Conclusions

We have investigated the one-photon photoluminescence properties of single gold nanoparticles by performing photothermal, fluorescence and dark-field scattering microscopy on the same individual particles. Our approach provides a direct measurement of the absorption cross section, emission intensities, and of the QY. We find that the QY of single gold nanorods with plasmon wavelengths longer than 650 nm is about an order of magnitude larger than that of single gold nanospheres. The observed QY is largely independent of the volume of nanorods, which is in agreement with our previous measurements on spheres. Over a broad spectral range, we find that the photoluminescence spectra closely resemble the scattering spectra, confirming the plasmonic nature of the emission. In the luminescence spectra, we find a weak, unpolarized component that we attribute to a combination of interband emission and transverse plasmon. Our results provide a better description and understanding of the photoluminescence of single gold nanoparticles and pave the way for their potential use in biological and soft matter studies. In our QY measurement, we excited the nanorods at 476 nm to reduce the effect of aspect ratio on the absorption cross sections. However, in a recent study the QY of a nanorod was reported to be even higher when excited on the blue wing of the longitudinal plasmon.[206] For future studies, it is therefore interesting to investigate the excitation wavelength dependence of the QY to obtain a complete picture of the luminescence mechanism. Here, we only studied one-photon luminescence properties of single gold nanorods. It would be interesting to investigate their QY and photoluminescence spectra upon two-photon excitation.

Acknowledgements

We acknowledge financial support by the ERC (Advanced Grant SiMoSoMa). This work is a part of the research program of the "Stichting voor Fundamenteel Onderzoek der Materie", which is financially supported by The Netherlands Organization for Scientific Research (NWO). Dr. Peter Zijlstra acknowledges financial support by NWO (Veni fellowship).